JOURNAL OF MOLECULAR SPECTROSCOPY **140,** 390–400 (1990)

High-Resolution Infrared Spectrum and Structure of Dinitrogen Sulfide, N_2S

R. D. BROWN, P. S. ELMES, AND D. MCNAUGHTON

Department of Chemistry, Monash University, Wellington Road, Clayton, Victoria, Australia 3168

The infrared spectrum of the ν_3 band of the transient molecule dinitrogen sulfide has been recorded at a resolution of 0.005 cm^{-1}. Analysis of the spectrum has been carried out using an interactive Loomis–Wood fitting program and the molecular constants and center frequencies of the cold bands due to $N_2{}^{32}S$ and $N_2{}^{34}S$ and four hot bands of $N_2{}^{32}S$ have been derived. The bond lengths of dinitrogen sulfide have been determined from the ground state constants of the two sulfur isotopomers to be r_{NN} = 113.876(19) pm and r_{NS} = 157.751(14) pm. The resultant geometry and frequencies are compared with the results of ab initio calculations and the geometries of similar molecules. © 1990 Academic Press, Inc.

Although many spectroscopic and structural data have been presented over the years on N_2O, it is only recently that its sulfur analog N_2S has been reported as an unstable product of the pyrolysis of 5-phenyl-1,2,3,4-thiatriazole(I). Despite earlier evidence to the contrary, Wentrup *et al.* (*1*) identified N_2S as a pyrolysis product from a band in the matrix isolation infrared spectrum of the pyrolytic products and from mass spectrometry. Bender *et al.* (*2*) subsequently confirmed the identification by recording the HeI photoelectron spectrum of the pyrolysate. We have employed the pyrolysis of I to generate N_2S in a flowthrough gas infrared cell and have recorded the ν_3 band at high resolution (0.005 cm^{-1}).

EXPERIMENTAL DETAILS

5-Phenyl-1,2,3,4-thiatriazole(I) (*3*) was vaporized at 100°C and pumped through a 300 × 25 mm quartz tube heated to 300°C directly into a multiple traversal infrared absorption cell set at 16 m path length. The cell was pumped continuously by a 200 liter min^{-1} two-stage rotary pump with an in-line cold trap held at −196°C. Spectra were recorded on a Bruker HR120 Fourier Transform infrared spectrometer (maximum resolution 0.0019 cm^{-1}) equipped with liquid nitrogen-cooled MCT (1800–650 cm^{-1}) and InSb (4000–1800 cm^{-1}) detectors and a helium-cooled bolometer (650–20 cm^{-1}).

Initial experiments at a variety of pumping speeds were carried out at a resolution of 1 cm^{-1} in an attempt to optimize the experimental conditions. Absorption bands of benzonitrile were easily identified in the pyrolysis products and a coating of sulfur rapidly appeared on the cell walls. During all flowthrough runs a further band not assignable to the precursor or to benzonitrile appeared at 2047 cm^{-1}, close to Wentrup's (*1*) matrix value of 2030 cm^{-1}. However upon isolation of the cell from the vacuum pump this band did not show any appreciable change in intensity over a period of 1

0022-2852/90 $3.00

hr. A high-resolution spectrum (0.002 cm^{-1}) of this stable gaseous species showed only a broad featureless band that we are unable to assign. Further flowthrough experiments were carried out at a resolution of 0.01 cm^{-1} and at the maximum pumping capacity of the system a new highly resolved spectrum showing rotational structure typical of a linear molecule was observed overlying the 2047 cm^{-1} band. This band has been assigned to the ν_3 vibration of N_2S. A further spectrum consisting of 20 computer averaged runs was recorded at a resolution of 0.005 cm^{-1} after the necessary inclusion of an optical filter (cut on at 2850 cm^{-1}). During the recording of the high-resolution spectra, which typically took 45 min, copious quantities of sulfur were deposited on the absorption cell walls, although the multireflection mirrors remained relatively free of deposits. Due to this deposition problem and the large amount of precursor material required for such high-resolution runs, no attempt was made to optimize the pyrolysis temperature.

The spectral line centers are presented as raw data from the Bruker peakfinder software. Only the wavenumbers of the centers of the assigned bands have been adjusted by calibrating lines of CO_2 (2345.0–2330.0 cm^{-1}) and H_2O (1920.0–1860.0 cm^{-1}) against the line centers of Guelachvili and Rao (*4*). The adjustment is +0.00197 cm^{-1}.

Ab initio calculations were carried out using the GAUSSIAN 88 (*5*) suite of programs on a VAX 8700 computer. All geometries were optimized at the appropriate basis set.

ASSIGNMENT AND DISCUSSION

The high-resolution spectrum presented in Fig. 1 was analyzed and assigned using MacLoomis (*6*), an interactive Loomis–Wood fitting program written at Monash University for Macintosh systems and based on a PC program recently described by Winnewisser *et al.* (*7*). Figure 2 shows a screen dump of an assignment of the *l* doubled hot hand (see below). Altogether nine bands have been identified using MacLoomis but only the lines of the most intense bands could originally be assigned

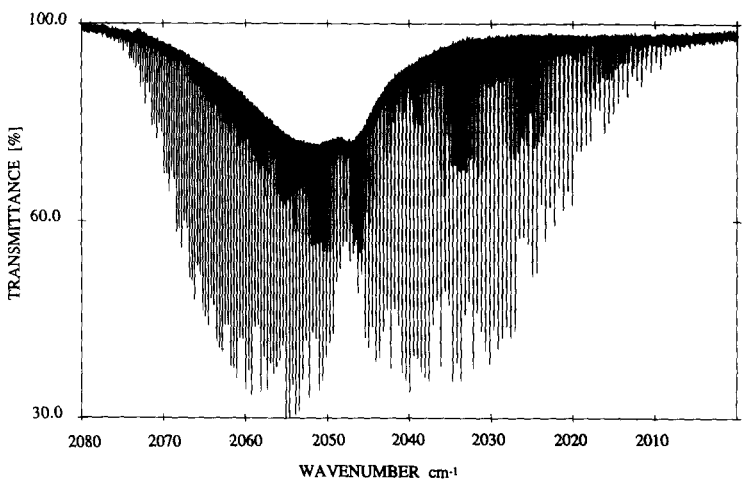

FIG. 1. High-resolution infrared spectrum of the ν_3 band of N_2S (0.005 cm^{-1}).

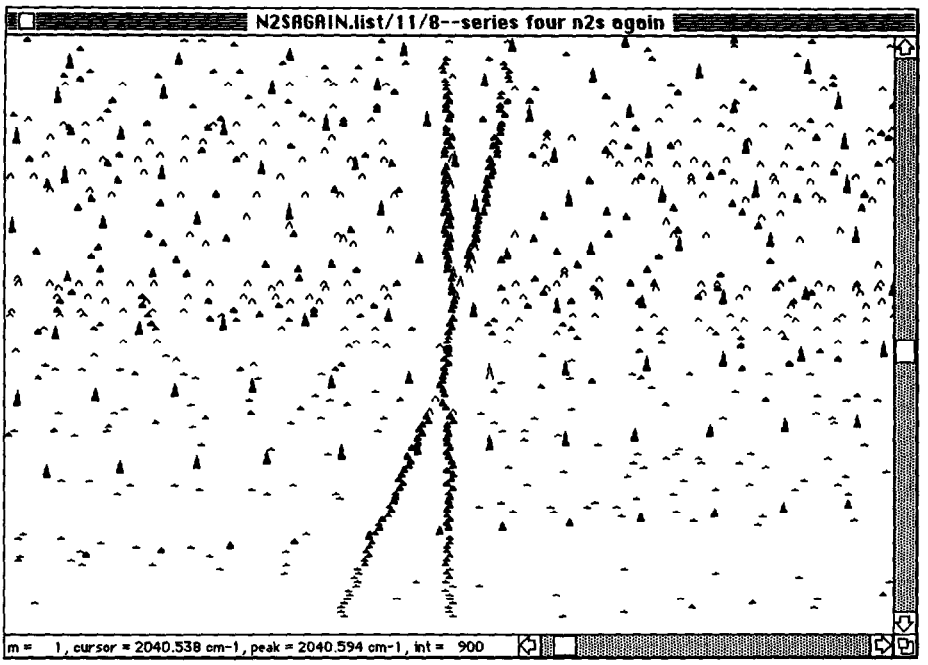

FIG. 2. MacLoomis plot showing the *l* doubled hot band emanating from ν_2. The doublet splitting is resolved at $J'' = 13$.

unique J values. The line positions for each of these bands (listed in Table I) were fitted to the expression for vibration–rotation bands of a linear molecule

$$\bar{\nu} = \bar{\nu}_0 + (B'' + B')m - (B'' - D'' - B' + D')m^2 - (2D'' - H'' + 2D' - H')m^3 + (D'' - 3H'' - D' + 3H')m^4 + 3(H'' + H')m^5 - (H'' - H')m^6,$$

where $m = -J''$ for P branches and $J'' + 1$ for R branches.

The resultant constants are listed in Table II. In all cases inclusion of the H centrifugal distortion terms resulted in only a small improvement in the standard deviation of the fit and lead to indeterminate values for H' and H''. The sets of lines marked in Table I were assigned unique J values only after the vibration–rotation parameters were first calculated from the more intense bands and subsequently used to obtain a consistent set of constants for all unperturbed bands. These assignments also resulted in a smaller sum of the squares of the errors in a least squares fit of the ground state combination differences compared to other J assignments. Two of the three hot bands emanating from $2\nu_2$, although assigned, have not been included as they are heavily perturbed by rotational *l* resonance.

COLD BANDS

The assignment and fitting of the most intense band in the spectrum leads to a B'' value for the ^{32}S isotopomer of 0.21643018(15) cm^{-1}. The expected B value of N_2S

TABLE I

Measured wavenumbers of the ν_3 Band of N_2S (cm^{-1})—The Values of the Running Constant m are $m = -J''$ for P branches and $m = J'' + 1$ for R branches

				$N_2{}^{32}S$ 3_0^1				
m	Observed	O - C	m	Observed	O - C	m	Observed	O - C
-73	2010.49493	0.00028	-21	2038.05223	-0.00033	31	2059.93902	-0.00001
-72	2011.07552	-0.00040	-20	2038.52832	0.00042	32	2060.30168	-0.00101
-71	2011.65585	0.00062	-19	2039.00047	-0.00066	33	2060.66359	-0.00057
-70	2012.23188	-0.00070	-18	2039.47168	-0.00058	34	2061.02366	0.00021
-69	2012.80745	-0.00052	-16	2040.40756	-0.00062	35	2061.38016	-0.00040
-68	2013.38175	0.00038	-15	2040.87331	0.00033	36	2061.73585	0.00036
-67	2013.95192	-0.00089	-14	2041.33499	-0.00066	37	2062.08750	-0.00074
-66	2014.52156	-0.00072	-13	2041.79577	-0.00044	38	2062.43820	-0.00060
-65	2015.09076	0.00101	-12	2042.25438	-0.00027	39	2062.78766	0.00048
-64	2015.65531	0.00006	-11	2042.71061	-0.00035	40	2063.13320	-0.00018
-63	2016.21956	0.00080	-10	2043.16466	-0.00050	41	2063.47796	0.00057
-62	2016.77947	-0.00082	-9	2043.61746	0.00023	42	2063.81858	-0.00064
-61	2017.33971	-0.00010	-8	2044.06747	0.00030	43	2064.15828	-0.00058
-60	2017.89662	-0.00073	-7	2044.51611	0.00113	44	2064.49696	0.00065
-59	2018.45425	0.00137	-6	2044.96064	-0.00002	45	2064.83153	-0.00006
-58	2019.00766	0.00125	-5	2045.40429	0.00008	46	2065.16540	0.00073
-57	2019.55717	-0.00077	-4	2045.84679	0.00117	47	2065.49499	-0.00057
-54	2021.19998	-0.00046	-3	2046.28573	0.00083	48	2065.82375	-0.00051
-53	2021.74315	-0.00076	-2	2046.72367	0.00163	49	2066.15171	0.00092
-52	2022.28481	-0.00055	-1	2047.15742	0.00038	50	2066.47493	-0.00018
-51	2022.82611	0.00132	1	2048.02180	0.00118	51	2066.79810	0.00084
-50	2023.36338	0.00120	2	2048.45051	0.00132	52	2067.11668	-0.00053
-49	2023.89721	-0.00033	3	2048.87702	0.00139	53	2067.43436	-0.00061
-48	2024.43193	0.00105	4	2049.29971	-0.00019	54	2067.75138	0.00083
-47	2024.96314	0.00096	5	2049.72163	-0.00040	55	2068.06386	-0.00008
-46	2025.49065	-0.00079	6	2050.14293	0.00091	56	2068.37607	0.00094
-45	2026.01967	0.00102	7	2050.55977	-0.00008	57	2068.68361	-0.00054
-44	2026.54345	-0.00038	8	2050.97590	0.00037	58	2068.99045	-0.00052
-43	2027.06727	0.00032	9	2051.38845	-0.00060	59	2069.29634	0.00075
-42	2027.58796	-0.00007	10	2051.80025	-0.00017	60	2069.59795	-0.00008
-41	2028.10793	0.00087	11	2052.20911	-0.00051	61	2069.89898	0.00070
-40	2028.62354	-0.00048	12	2052.61636	-0.00032	62	2070.19580	-0.00054
-39	2029.13857	-0.00036	13	2053.02138	-0.00019	63	2070.49175	-0.00046
-38	2029.65247	0.00068	14	2053.42470	0.00040	64	2070.78649	0.00060
-37	2030.16273	0.00016	15	2053.82489	0.00002	65	2071.07705	-0.00033
-36	2030.67194	0.00065	16	2054.22406	0.00078	66	2071.36728	0.00060
-35	2031.17716	-0.00079	17	2054.61938	-0.00014	67	2071.65350	-0.00030
-34	2031.68172	-0.00081	18	2055.01371	0.00011	68	2071.93856	-0.00016
-33	2032.18461	-0.00043	19	2055.40550	-0.00000	69	2072.22199	0.00053
-32	2032.68478	-0.00069	20	2055.79552	0.00028	70	2072.50177	-0.00023
-31	2033.18301	-0.00082	21	2056.18208	-0.00073	71	2072.78074	0.00038
-30	2033.68004	-0.00006	22	2056.56821	-0.00000	72	2073.05732	0.00079
-29	2034.17363	-0.00067	23	2056.95210	0.00065	73	2073.33018	-0.00034
-28	2034.66624	-0.00016	24	2057.33181	-0.00071	74	2073.60275	0.00044
-27	2035.15587	-0.00055	25	2057.71061	-0.00078	75	2073.87153	-0.00039
-26	2035.64421	-0.00014	26	2058.08760	-0.00051	76	2074.13941	0.00007
-25	2036.12955	-0.00063	27	2058.46246	-0.00018	77	2074.40498	0.00040
-24	2036.61361	-0.00032	28	2058.83467	-0.00034	79	2074.92878	0.00028
-23	2037.09496	-0.00061	29	2059.20500	-0.00020	80	2075.18646	-0.00072
-22	2037.57526	0.00014	30	2059.57269	-0.00051	81	2075.44290	-0.00078

can be derived by scaling the equilibrium B value calculated from an ab initio geometry optimization with a factor calculated from the ratio of $B_{exp}/B_{ab\ initio}$ for related molecules. With MP3/6-31G* basis sets these predictions have been found to be good to within 1% or better. For the ab initio geometries presented in Table III the appropriate calculations using N_2O and OCS as scaling molecules give a B value of 0.2152 cm^{-1}

TABLE I—*Continued*

				$N_2{}^{34}S$ 3_0^1				
m	Observed	O - C	*m*	Observed	O - C	*m*	Observed	O - C
-51	2023.25387	0.00036	-18	2039.48668	-0.00120	27	2058.01720	-0.00118
-50	2023.77676	-0.00070	-15	2040.85615	0.00197	29	2058.74435	0.00101
-49	2024.29997	0.00051	-14	2041.30620	0.00070	30	2059.10112	-0.00154
-48	2024.81996	0.00049	-13	2041.75510	0.00034	31	2059.45946	-0.00038
-47	2025.33600	-0.00150	-12	2042.20233	0.00037	32	2059.81366	-0.00125
-46	2025.85260	-0.00096	-11	2042.64811	0.00102	33	2060.16877	0.00090
-44	2026.88067	0.00096	-10	2043.09202	0.00186	34	2060.51926	0.00054
-43	2027.39039	0.00059	-9	2043.53059	-0.00059	35	2060.86549	-0.00194
-42	2027.89819	0.00029	-8	2043.96919	-0.00092	36	2061.21505	0.00102
-41	2028.40409	0.00009	-7	2044.40722	0.00024	37	2061.55950	0.00099
-40	2028.90820	0.00010	-4	2045.70586	0.00070	38	2061.90020	-0.00067
-39	2029.41108	0.00088	-3	2046.13173	-0.00200	39	2062.23994	-0.00117
-38	2029.91048	0.00018	-2	2046.55971	-0.00051	40	2062.57946	0.00024
-37	2030.40913	0.00074	3	2048.66227	0.00079	41	2062.91404	-0.00117
-36	2030.90330	-0.00118	4	2049.07471	-0.00077	42	2063.24818	-0.00090
-35	2031.39795	-0.00060	5	2049.48629	-0.00110	43	2063.58176	0.00093
-34	2031.88921	-0.00141	6	2049.89664	-0.00056	44	2063.91066	0.00021
-33	2032.38129	0.00063	7	2050.30473	-0.00019	45	2064.23925	0.00130
-32	2032.86928	0.00059	8	2050.71196	0.00140	46	2064.56293	-0.00040
-31	2033.35582	0.00112	9	2051.11323	-0.00087	47	2064.88612	-0.00046
-30	2033.83864	-0.00004	12	2052.31290	0.00076	48	2065.20906	0.00136
-29	2034.32080	0.00017	13	2052.70750	0.00021	49	2065.52686	0.00016
-28	2034.80029	-0.00028	14	2053.10148	0.00114	50	2065.84456	0.00099
-27	2035.27963	0.00116	15	2053.49083	-0.00046	53	2066.78161	0.00017
-25	2036.22759	-0.00058	16	2053.87966	-0.00048	54	2067.08894	-0.00087
-24	2036.69897	-0.00101	17	2054.26803	0.00115	56	2067.70128	0.00110
-23	2037.16950	-0.00023	18	2054.65203	0.00051	57	2068.00276	0.00058
-22	2037.63653	-0.00092	19	2055.03518	0.00113	58	2068.29974	-0.00229
-21	2038.10211	-0.00102	23	2056.54246	-0.00065	59	2068.59940	-0.00038
-20	2038.56680	0.00004	25	2057.28476	-0.00021	60	2068.89614	0.00075
-19	2039.02746	-0.00088	26	2057.65374	0.00101			

for N_2S, thus confirming that the transient molecule under investigation is indeed N_2S.

The cold band emanating from the ^{34}S isotopomer is also identifiable in the spectrum. After elimination of the bands affected by *l* doubling (see below) there are four remaining bands with the intensity expected for the ^{34}S species. One of these has not been uniquely assigned but its center is some 15 cm^{-1} lower than that of the ^{32}S species. The ν_3 band under investigation is principally due to the N–N stretch and hence the band center of the ^{34}S species should be very close to that of the ^{32}S species, albeit a little lower. (Ab initio frequency calculations using force constants derived at the HF/6-31G* level result in identical frequencies for the two species.) This band may be ruled out on these grounds alone. Of the three remaining bands two have centers more than 1 cm^{-1} higher than that of the ^{32}S species and the third has its center 0.2 cm^{-1} lower. The two at higher wavenumbers are thus unlikely contenders and also have B'' values that are incompatible with that expected for the ^{34}S isotopomer. The expected B'' value may be calculated from the MP3/6-31G* ab initio geometry and after scaling by the ratio of $^{32}B_{exp}/^{32}B_{ab\ initio}$ gives a value of 0.21112 cm^{-1}. The third band results in a B'' value of 0.2111677(40) cm^{-1}, in excellent agreement with that expected for the ^{34}S isotopomer. The other bands have been assigned to hot bands as outlined below.

TABLE I—*Continued*

$N_2{}^{32}S$ $3_0^1 2_1^{1e}$

m	Observed	O - C	m	Observed	O - C	m	Observed	O - C
-60	2010.45044	0.00055	-20	2031.10105	-0.00074	22	2049.24046	-0.00042
-59	2011.00475	-0.00033	-19	2031.57623	-0.00026	23	2049.62878	0.00140
-58	2011.55769	-0.00061	-18	2032.04796	-0.00115	24	2050.01226	0.00052
-57	2012.11085	0.00129	-17	2032.51864	-0.00104	26	2050.77363	-0.00046
-56	2012.65867	-0.00019	-16	2032.98940	0.00123	27	2051.15156	-0.00050
-55	2013.20625	0.00006	-15	2033.45516	0.00056	28	2051.52926	0.00137
-54	2013.75009	-0.00146	-14	2033.92049	a	29	2051.90190	0.00031
-53	2014.29626	0.00132	-13	2034.37980	a	30	2052.27450	0.00135
-52	2014.83501	-0.00134	-12	2034.83887	a	31	2052.64170	-0.00089
-51	2015.37610	0.00031	-11	2035.29398	a	32	2053.01046	0.00059
-50	2015.91284	-0.00041	-10	2035.75335	a	33	2053.37544	0.00041
-49	2016.44958	0.00086	-9	2036.20717	a	34	2053.73724	-0.00079
-48	2016.98137	-0.00083	-8	2036.65770	a	35	2054.09868	-0.00022
-47	2017.51321	-0.00048	-7	2037.10891	a	36	2054.45661	-0.00102
-46	2018.04389	0.00069	-6	2037.55655	a	38	2055.16744	-0.00121
-45	2018.57014	-0.00056	-5	2038.00279	a	39	2055.52109	0.00014
-44	2019.09594	-0.00026	-4	2038.44658	a	40	2055.87005	-0.00104
-43	2019.62068	0.00097	-3	2038.88951	-0.00007	41	2056.21891	-0.00020
-42	2020.14197	0.00076	-2	2039.32730	-0.00163	44	2057.24900	-0.00126
-40	2021.17797	-0.00021	-1	2039.76641	0.00023	45	2057.58871	-0.00097
-39	2021.69309	-0.00056	2	2041.06475	-0.00059	46	2057.92796	0.00100
-38	2022.20749	0.00038	3	2041.49429	0.00011	47	2058.26223	0.00015
-37	2022.71777	-0.00077	4	2041.92101	0.00008	48	2058.59664	0.00158
-36	2023.22715	-0.00081	5	2042.34716	a	49	2058.92528	-0.00061
-35	2023.73619	0.00084	6	2042.76931	a	50	2059.25412	-0.00045
-34	2024.24053	-0.00019	7	2043.19060	a	52	2059.90619	0.00071
-33	2024.74444	0.00038	9	2044.02470	a	53	2060.22869	0.00098
-32	2025.24494	-0.00043	10	2044.43970	a	54	2060.54735	-0.00044
-31	2025.74602	0.00138	11	2044.85206	a	56	2061.18228	0.00080
-30	2026.24085	-0.00103	12	2045.26271	a	57	2061.49472	-0.00039
-29	2026.73827	0.00118	13	2045.66892	a	58	2061.80742	0.00084
-28	2027.23163	0.00139	14	2046.07410	a	59	2062.11564	-0.00025
-27	2027.72064	-0.00072	15	2046.48124	a	60	2062.42300	-0.00006
-26	2028.21182	0.00139	16	2046.87947	a	61	2062.72760	-0.00047
-25	2028.69838	0.00091	17	2047.27937	a	63	2063.33068	-0.00097
-24	2029.18217	-0.00027	18	2047.67396	a	64	2063.62932	-0.00089
-23	2029.66465	-0.00071	19	2048.06914	0.00052	65	2063.92712	0.00051
-22	2030.14630	0.00007	20	2048.46228	0.00078	66	2064.22174	0.00089
-21	2030.62426	-0.00079	21	2048.85237	0.00012			

a. Doublets not included in the fit.

HOT BANDS

The hot bands have been assigned by comparison of their relative intensities (using the frequencies from the HF/6-31G* calculation to derive the Boltzmann factors), the use of symmetry arguments and comparison of the B values. The two most intense bands after the ^{32}S species cold band arise from almost the same center frequency and so are easily assigned as belonging to the II–II transition emanating from the bending mode, i.e., $\nu_2 + \nu_3 \leftarrow \nu_2$. The l doubling splitting is resolved at $J = 13$ as is easily seen in the screen dump of the MacLoomis fit of Fig. 2. From the values of B^e and B^f in Table II the value of q_2, the l doubling constant, is calculated to be 0.0002714(72) cm^{-1}. From the approximate expression for q_2 (ignoring Coriolis coupling) $q_2 = 2B_e^2/\omega_2$ (where B_e is calculated from the vibration–rotation parameters—see below) the location of the bending mode is calculated to be $\approx$343 cm^{-1} somewhat lower

TABLE I—*Continued*

$N_2{}^{32}S$ $3_0^1 2_1^{1f}$

m	Observed	O - C	m	Observed	O - C	m	Observed	O - C
-60	2010.40657	0.00205	-21	2030.61203	0.00071	25	2050.40618	0.00079
-59	2010.96047	-0.00020	-20	2031.08882	0.00009	26	2050.78560	-0.00033
-58	2011.51399	-0.00086	-19	2031.56564	0.00155	27	2051.16428	-0.00006
-57	2012.06683	-0.00023	-18	2032.03709	-0.00029	28	2051.54037	-0.00022
-56	2012.61753	0.00023	-17	2032.50837	-0.00022	29	2051.91426	-0.00046
-55	2013.16596	0.00039	-16	2032.97958	0.00185	30	2052.28596	-0.00074
-54	2013.71071	-0.00113	-15	2033.44526	0.00047	31	2052.65766	0.00112
-53	2014.25747	0.00132	-14	2033.91080	a	33	2053.39123	0.00143
-52	2014.79945	0.00098	-11	2035.29398	a	34	2053.75357	0.00036
-51	2015.33770	-0.00110	-10	2035.75335	a	35	2054.11506	0.00058
-50	2015.87720	0.00005	-9	2036.20717	a	36	2054.47317	-0.00043
-49	2016.41216	-0.00134	-8	2036.65770	a	37	2054.83085	0.00028
-48	2016.94829	0.00044	-7	2037.10891	a	38	2055.18467	-0.00073
-47	2017.47982	-0.00038	-6	2037.55655	a	39	2055.53914	0.00105
-46	2018.01109	0.00053	-5	2038.00279	a	40	2055.88983	0.00121
-45	2018.53772	-0.00118	-4	2038.44658	a	41	2056.23605	-0.00095
-44	2019.06410	-0.00115	-3	2038.88951	a	42	2056.58282	-0.00041
-43	2019.58915	-0.00044	-2	2039.32730	0.00041	43	2056.92627	-0.00105
-41	2020.63108	-0.00113	-1	2039.76641	0.00171	44	2057.27073	0.00147
-40	2021.15037	-0.00013	2	2041.06475	-0.00075	45	2057.61020	0.00116
-39	2021.66606	-0.00070	3	2041.49429	-0.00060	46	2057.94567	-0.00101
-38	2022.18049	-0.00052	4	2041.92101	-0.00116	47	2058.28285	0.00070
-37	2022.69435	0.00112	5	2042.34716	-0.00018	48	2058.61431	-0.00117
-36	2023.20455	0.00113	6	2042.76931	-0.00109	49	2058.94717	0.00052
-35	2023.71124	-0.00034	7	2043.19060	-0.00074	50	2059.27583	0.00016
-34	2024.21854	0.00083	9	2044.02470	a	51	2059.60335	0.00081
-33	2024.72247	0.00067	10	2044.43970	a	53	2060.25079	0.00098
-32	2025.22372	-0.00014	11	2044.85206	a	54	2060.56927	-0.00094
-31	2025.72477	0.00090	12	2045.26271	a	55	2060.88710	-0.00137
-30	2026.22308	0.00122	13	2045.66892	a	56	2061.20593	0.00137
-29	2026.71679	-0.00099	14	2046.07410	a	57	2061.51700	-0.00150
-28	2027.21069	-0.00097	15	2046.48124	a	58	2061.82904	-0.00124
-27	2027.70297	-0.00052	18	2047.68277	a	61	2062.75377	0.00108
-26	2028.19383	0.00056	19	2048.07712	-0.00020	62	2063.05627	0.00043
-25	2028.68180	0.00080	21	2048.86078	-0.00109	63	2063.35741	0.00056
-24	2029.16564	-0.00102	22	2049.25001	-0.00094	64	2063.65480	-0.00090
-22	2030.13096	-0.00086	24	2050.02276	0.00005			

a Doublets not included in the fit.

than the value of 424 cm^{-1} from the scaled ab initio calculation. This value does, however, confirm the assignment.

The next most intense band in the spectrum is a single band with no apparent l doubling, which is compatible in intensity with a hot band arising from ν_1, the N–S stretch, i.e., $\nu_1 + \nu_3 \leftarrow \nu_1$. The lack of l doubling indicates the band is from a $\Sigma-\Sigma$ transition as expected for this hot band and the B'' value of 0.2158475(84) cm^{-1} is smaller than that of the cold band as would be expected for a stretching mode where the bond lengths are increased relative to the ground state.

The next most intense band should emanate from $2\nu_2$ and give rise to a $\Delta-\Delta$ band and a $\Sigma-\Sigma$ band. Three bands centered approximately 14.7 cm^{-1} below the cold band have the correct relative intensities with a pair of bands showing l doubling and the remaining band showing no doubling. The center of the ν_2 hot band is 7.4 cm^{-1} below that of the cold band; hence these three bands are in the expected position for the overtone hot band and can be assigned to $2\nu_2$. The $\Sigma-\Sigma$ band with $l = 0$ and the l

TABLE I—*Continued*

$N_2{}^{32}S$ $3_0^1 1_1^1$

m^a	Observed	O - C	m	Observed	O - C	m	Observed	O - C
-46	2027.76792	0.00176	-17	2042.16118	-0.00100	28	2061.04563	0.00139
-45	2028.28946	-0.00156	-16	2042.62698	-0.00086	29	2061.41441	-0.00071
-44	2028.81478	0.00092	-14	2043.55277	-0.00020	30	2061.78525	0.00140
-42	2029.85237	-0.00113	-12	2044.46973	-0.00007	31	2062.15177	0.00133
-41	2030.37082	0.00054	-11	2044.92692	0.00182	32	2062.51393	-0.00096
-40	2030.88486	-0.00019	-6	2047.17109	0.00069	33	2062.87585	-0.00134
-38	2031.91005	0.00154	-5	2047.61314	-0.00007	34	2063.23777	0.00043
-37	2032.41522	-0.00197	2	2050.65303	-0.00126	35	2063.59507	-0.00027
-36	2032.92351	-0.00034	6	2052.34582	-0.00005	36	2063.95052	-0.00067
-35	2033.42816	-0.00032	7	2052.76257	-0.00093	37	2064.30533	0.00045
-34	2033.93176	0.00068	8	2053.17779	-0.00124	38	2064.65617	-0.00025
-33	2034.43065	-0.00099	9	2053.59398	0.00154	39	2065.00673	0.00092
-32	2034.92937	-0.00078	10	2054.00552	0.00178	40	2065.35250	-0.00053
-31	2035.42762	0.00098	11	2054.41237	-0.00057	41	2065.69750	-0.00060
-30	2035.92071	-0.00037	13	2055.22660	0.00164	42	2066.04209	0.00108
-29	2036.41379	0.00032	14	2055.62754	-0.00026	43	2066.38194	0.00019
-28	2036.90280	-0.00102	15	2056.02742	-0.00110	44	2066.72187	0.00153
-27	2037.39227	0.00014	16	2056.42710	-0.00001	45	2067.05617	-0.00059
-26	2037.87726	-0.00112	17	2056.82326	-0.00033	47	2067.72312	0.00001
-25	2038.36351	0.00092	18	2057.21701	-0.00093	50	2068.70598	-0.00038
-24	2038.84605	0.00131	20	2057.99981	-0.00045	51	2069.02871	-0.00106
-22	2039.80431	0.00143	22	2058.77305	-0.00101	52	2069.35105	0.00005
-21	2040.27851	-0.00035	23	2059.15731	-0.00046	53	2069.67023	0.00017
-20	2040.75273	-0.00006	24	2059.53906	-0.00027	57	2070.92468	0.00015
-18	2041.69522	0.00077	25	2059.91949	0.00072			

$N_2{}^{32}S$ $3_0^1 1_2^2$

m^a	Observed	O - C	m	Observed	O - C	m	Observed	O - C
-38	2028.77177	-0.00090	-10	2042.22697	-0.00000	25	2056.73932	-0.00170
-37	2029.28310	0.00247	-8	2043.12434	-0.00173	26	2057.11743	0.00006
-33	2031.29112	-0.00129	-7	2043.57178	-0.00071	27	2057.48987	-0.00173
-32	2031.78940	-0.00092	-4	2044.89978	0.00065	28	2057.86320	-0.00048
-31	2032.28428	-0.00193	-1	2046.20577	-0.00109	31	2058.96607	-0.00100
-30	2032.78131	0.00123	9	2050.42945	0.00083	22	2059.33073	0.00014
-29	2033.27198	0.00007	10	2050.83998	0.00085	23	2059.69162	-0.00033
-28	2033.76080	-0.00092	11	2051.24581	-0.00171	34	2060.05204	0.00086
-27	2034.24934	-0.00014	12	2051.65424	0.00047	35	2060.40986	0.00159
-26	2034.73669	0.00148	14	2052.46024	0.00033	36	2060.76268	-0.00053
-25	2035.21874	-0.00015	15	2052.86022	0.00044	37	2061.11687	0.00087
-24	2035.70136	0.00083	16	2053.25902	0.00150	42	2062.84828	0.00041
-23	2036.17989	-0.00024	19	2054.43855	0.00064	43	2063.18747	-0.00034
-21	2037.13249	-0.00066	22	2055.59940	0.00031	45	2063.86100	-0.00029
-20	2037.60821	0.00164	23	2055.98258	0.00071	46	2064.19472	-0.00010
-19	2038.07898	0.00105	24	2056.36199	-0.00053			

a. These m values have been assigned to give B values consistent with those calculated from the α_i constants.

$= +2$ component of the $\Delta-\Delta$ band are heavily perturbed by rotational l resonance, which cannot be treated by the simple approach we have taken. Hence only the $l = -2$ component of the $\Delta-\Delta$ band, which is not perturbed, is presented. The ninth and weakest band in the spectrum on intensity arguments must emanate from $\nu_2 + \nu_1$ or possibly $2\nu_1$. Both would be centered close to the cold band. The weakest band in the spectrum shows no doubling and is close to the cold band center. Hence it probably arises from $2\nu_1$ because $\nu_2 + \nu_1$, being a $\Pi-\Pi$ band, would be expected to show l doubling. The $\nu_2 + \nu_1$ is probably not observed because its intensity would be distributed over the two l components of the band.

TABLE I—*Continued*

$N_2{}^{32}S$ $3_0^1 2_2^{2f}$

m[a]	Observed	O - C	m	Observed	O - C	m	Observed	O - C
-36	2015.84662	-0.00050	-12	2027.50593	b			
-35	2016.35598	0.00005	-11	2027.96715	b	19	2040.82458	b
-34	2016.86247	-0.00027	-10	2028.42724	b	21	2041.61283	b
-32	2017.86957	-0.00086	-9	2028.88325	0.00186	22	2042.00714	0.00076
-31	2018.37266	0.00137	-8	2029.33538	-0.00038	23	2042.39602	-0.00051
-30	2018.87160	0.00145	-7	2029.78730	-0.00079	24	2042.78465	0.00012
-29	2019.36597	-0.00105	-6	2030.23933	0.00096	27	2043.93618	0.00028
-28	2019.86307	0.00117	-5	2030.68542	-0.00117	28	2044.31385	-0.00166
-27	2020.35639	0.00162	-4	2031.13250	-0.00027	29	2044.69202	-0.00101
-26	2020.84461	-0.00103	-2	2032.02031	0.00137	30	2045.06919	0.00074
-24	2021.81926	-0.00209	5	2035.05560	0.00009	31	2045.44254	0.00078
-23	2022.30618	0.00001	6	2035.48266	0.00161	32	2045.81427	0.00129
-22	2022.78856	-0.00046	7	2035.90451	0.00002	33	2046.18212	0.00003
-21	2023.27095	0.00116	8	2036.32504	-0.00083	34	2046.55027	0.00116
-20	2023.74790	-0.00073	9	2036.74313	-0.00203	35	2046.91337	-0.00065
-18	2024.70012	0.00003	13	2038.40217	b	37	2047.63702	-0.00050
-17	2025.17174	-0.00113	14	2038.81035	b	38	2047.99536	-0.00077
-16	2025.64353	0.00003	15	2039.21847	b	39	2048.35199	-0.00063
-15	2026.11254	0.00033	16	2039.62223	b	40	2048.70846	0.00145
-14	2026.58015	b	17	2040.02613	b	41	2049.05882	-0.00047

a. These m values have been assigned to give B values consistent with those calculated from the α_i constants.

b. Doublets not included in the fit.

TABLE II

Rotational and Centrifugal Distortion Constants of the Assigned Vibrational Bands of N_2S (cm^{-1})

	$^{32}S\ 3_0^1$	$^{34}S\ 3_0^1$	$^{32}S\ 3_0^1 1_1^1$	$^{32}S\ 3_0^1 1_2^2$
$\bar{\nu}_0$[a]	2047.591873(98)	2047.40897(20)	2049.79785(24)	2046.64066(38)
B''	0.2164302(15)	0.2111677(40)	0.2161738(49)	0.215847(84)
D''	6.543(20) × 10^{-8}	6.275(104)× 10^{-8}	7.004(155)× 10^{-8}	7.771(392)× 10^{-8}
B'	0.2153589(15)	0.2101264(39)	0.2151253(48)	0.2147920(82)
D'	6.654(20)× 10^{-8}	6.386(110)× 10^{-8}	7.035(167)× 10^{-8}	8.015(426)× 10^{-8}

	$^{32}S\ 3_0^1 2_1^{1e}$	$^{32}S\ 3_0^1 2_1^{1f}$	$^{32}S\ 3_0^1 2_2^{2f}$	vibration-rotation constants[b]
$\bar{\nu}_0$	2040.20330(22)	2040.20237(23)	2032.89883(30)	α_1 0.256(6) × 10^{-3}
B''	0.2175763(29)	0.2178537(32)	0.2189661(88)	α_2 -1.285(6) × 10^{-3}
D''	6.844(54)× 10^{-8}	6.644(62)× 10^{-8}	7.190(427)× 10^{-8}	α_3 1.071(3) × 10^{-3}
B'	0.2165226(28)	0.2168016(32)	0.2179342(86)	
D'	6.950(56)× 10^{-8}	6.752(64)× 10^{-8}	7.344(460)× 10^{-8}	

[a] From calibration data all center frequencies have been adjusted by +0.00197 cm^{-1} (see text).
[b] Derived from the B values of the ground state, 3_1, 2_1, and 1_1.

TABLE III

Geometric Parameters of N_2S and Related Molecules (pm)

	HF/6-31G*	MP3/6-31G*	r_0	Partial r_s
N_2S				
r_{NN}	108.60	112.529	113.876(19)	113.877
r_{NS}	165.20	159.816	157.751(14)	157.750
			Expl[a]	
OCS				
r_{CO}	113.12	115.869	115.7	
r_{CS}	157.25	156.677	156.1	
N_2O				
r_{NN}	109.210	112.626	112.86	
r_{NO}	117.830	119.295	118.76	

a. Geometries from reference (8)

From the four sets of rotational constants for the ground state, ν_1, ν_2, and ν_3, the vibration–rotation constants in Table II have been calculated from

$$B_v = B_e - \sum_i \alpha_i \left[v_i + \frac{d_i}{2} \right].$$

The equilibrium B value is then calculated to be 0.215809(17) cm^{-1}, which is within 0.5% of that calculated from the MP3/6-31G* optimized geometry (0.21456 cm^{-1}). From this value of B_e and the calculated α_i values the B_v values for $2\nu_1$, $\nu_1 + \nu_3$, $\nu_2 + \nu_3$, and $2\nu_2$ have been estimated. All four estimated values of B_v are within 5×10^{-5}

TABLE IV

Vibrational Frequencies of N_2S and Related Molecules (cm^{-1})

	HF/6-31G*	Scaled by 0.9	Experimental	Calc. Intensity
N_2S				
ν_2	470.8	424.	343.[a]	3.3
ν_1	582.6	525.		44.7
ν_3	2597.4	2237.	2047.59	295.
OCS				
ν_2	566.2	510.	520.4	
ν_1	888.6	800.	858.9	
ν_3	2306.8	2076.	2062.9	
N_2O				
ν_2	689.0	620.	589.	
ν_1	1394.2	1255.	1285.	
ν_3	2633.2	2370.	2224.	

a. Approximate frequency from B_e.

cm^{-1} of the values in Table II. This consistency of results is the final confirmation of our band assignments and J numbering.

From the ground state rotational constants of the two sulfur species the geometry of dinitrogen sulfide has been calculated. An r_0 structure has been derived by a least-square fit of the rotational constants and a partial r_s structure has been calculated by using Kraitchman's equations to determine the position of the sulfur and the first and second moment equations to determine the nitrogen positions. These two calculated geometries are presented in Table III, together with the results of the ab initio calculations and the geometries of the related molecules N_2O and OCS. The two calculated geometries are almost identical and both bond lengths, as expected from the comparison calculations, are slightly shorter than the equilibrium bond lengths predicted by the MP3/6-31G* calculations. The N–N bond length of 113.88 pm is 1 pm longer than that in N_2O, whilst the N–S bond length of 157.75 pm is much longer than the N–S bond of 151.1 pm in HNSO (*8*). The geometric parameters are very similar to those of OCS.

The calculated vibrational frequencies of N_2S shown in Table IV are unusual in that, unlike OCS and N_2O, where the generally accepted scaling factor of 0.9 yields results consistent with experiment, the N–N stretch frequency is much lower than expected. It is, however, very similar to the asymmetric stretch frequency in OCS, which from the similarities in geometry, atom size, and electronegativities of the two molecules might be expected. Attempts to observe the ν_1 and ν_2 bands of N_2S have so far proved unsuccessful. Both of these bands are significantly less intense than ν_3 and this, together with the less sensitive detector in the far infrared region, makes their detection difficult.

RECEIVED: December 20, 1989

REFERENCES

1. C. WENTRUP, S. FISCHER, A. MAQUESTIAU, AND R. FLAMMANG, *J. Org. Chem.* **51,** 1908–1910 (1986).
2. H. BENDER, F. CARNOVALE, J. BARRIE PEEL, AND C. WENTRUP, *J. Amer. Chem. Soc.* **110,** 3458–3461 (1988).
3. E. LIEBER, C. N. R. RAO, AND R. C. ORLOWSKI, *Canad. J. Chem.* **41,** 926–931 (1963).
4. G. GUELACHVILI AND K. NARAHARI RAO, "Handbook of Infrared Standards," Academic Press, New York, 1986.
5. M. J. FRISCH, M. HEAD-GORDON, H. B. SCHLEGEL, K. RAGHAVACHARI, J. S. BINKLEY, C. GONZALEZ, D. J. DEFREES, D. J. FOX, R. A. WHITESIDE, R. SEEGER, C. F. MELIUS, J. BAKER, R. L. MARTIN, R. L. KAHN, J. J. P. STEWART, E. M. FLUDER, S. TOPIOL AND J. A. POPLE, "GAUSSIAN 88," Gaussian, Inc., Pittsburgh, 1988.
6. D. MCGILVERY AND D. MCNAUGHTON, to be published.
7. B. P. WINNEWISSER, J. REINSTADTLER, K. M. T. YAMADA, AND J. BEHREND, *J. Mol. Spectrosc.* **136,** 12–16 (1989).
8. M. D. HARMONY, V. W. LAURIE, R. L. KUCZKOWSKI, R. H. SCHWENDEMAN, D. A. RAMSAY, F. J. LOVAS, W. J. LAFFERTY, AND A. G. MAKI, *J. Phys. Chem. Ref. Data* **15,** 619–721 (1979).